Electronic Supplementary Information

Planarized *B*-Phenylborataanthracene Anion: Structural and Electronic Impacts of Coplanar-Constraint

Tomokatsu Kushida,[a] Zhiguo Zhou,[a] Atsushi Wakamiya,[b] and Shigehiro Yamaguchi*[a]

[a] *Department of Chemistry, Graduate School of Science, Nagoya University, and CREST, Japan Science and Technology Agency, Furo, Chikusa, Nagoya 464-8602, Japan*
[b] *Institute for Chemical Research, Kyoto University*

E-mail: yamaguchi@chem.nagoya-u.ac.jp

Contents

1. Experimental Details

General. Melting points (mp) were determined with a Yanaco MP-S3 instrument. ^{1}H, ^{13}C, ^{7}Li, and ^{11}B NMR spectra were measured with a JEOL AL-400 spectrometer (400 MHz for ^{1}H, 100 MHz for ^{13}C, 155 MHz for [7]Li, and 128 MHz for [11]B) in sealed tube in THF-d_8 that was dried over sodium-potassium (NaK) alloy and degassed by Freeze-Pump-Thaw cycles. Chemical shifts are reported in δ ppm. ^{1}H NMR spectra are referenced to residual protons in the deuterated solvent; ^{13}C NMR spectra are referenced to carbon-13 in the deuterated solvent; ^{7}Li NMR spectrum is referenced to LiCl as an external standard; ^{11}B NMR spectra are referenced to BF$_3$·OEt$_2$ as an external standard. THF and hexane were distilled over sodium-benzophenone ketyl or calcium hydride and degassed by Freeze-Pump-Thaw cycles. Planarized triphenylborane **1** was prepared as described in the literature.[1] All reactions were carried out under an argon (Ar) or a nitrogen (N$_2$) atmosphere.

Potassium salt of planarized *B*-phenylborataanthracene 2·K. To a solution of planarized triphenylborane **1** (50.5 mg, 0.15 mmol) in THF (5 mL) was added potassium hydride (6.6 mg, 0.16 mmol) at room temperature. After stirring for 24 h, the resulting red solution was filtered off and concentrated under reduced pressure. Recrystallization from THF with slow diffusion of a hexane solution of [2.2.2]cryptand (57.0 mg, 0.15 mmol) gave 73.7 mg (0.098 mmol) of **2·K** in 66% yield as red crystals: mp 172-180 °C (dec.); ^{1}H NMR (400 MHz, THF-d_8) δ 1.65 (s, 12H), 2.01 (t, ^3J = 4.8 Hz, 12H), 3.00 (t, ^3J = 4.8 Hz, 12H), 3.08 (s, 12H), 6.64 (d, ^3J = 6.8 Hz, 2H), 6.77 (s, 1H), 7.01-7.07 (m, 3H), 7.21 (d, ^3J = 8.4 Hz, 2H), 7.29 (d, ^3J = 8.4 Hz, 2H); ^{13}C NMR (100 MHz, THF-d_8) δ 36.1 (q), 42.7 (s), 54.2 (t), 67.9 (t), 70.7 (t), 102.5 (d), 109.5 (d), 122.4 (d), 122.9 (d), 125.7 (d), 126.2 (d), 141.1 (s), 152.7 (s), 154.7 (s), two signals for the carbon atoms bound to the boron atom were not observed due to the quadrupolar relaxation; ^{11}B NMR (128 MHz, THF-d_8) δ 30.0. The elemental analysis could not be performed due to the instability of the product toward air and moisture.

**Lithium salt of planarized *B*-phenylborataanthracene 2·Li.** To a solution of tetramethylpiperidine (20 μL, 0.12 mmol) in THF (1 mL) was added a hexane solution of *n*-BuLi (1.6 M, 75 μL, 0.12 mmol) at 0 °C. After stirring for 1 h at 0 °C, the solution was added to a solution of planarized triphenylborane **1** (39.8 mg, 0.12 mmol) in THF (3 mL), then stirred for 1 h at 0 °C. The volatile materials were removed in vacuo at room temperature. Recrystallization from THF with slow diffusion of hexane under an argon atmosphere gave 49.3 mg (0.078 mmol) of **2·Li** in 66% yield as red crystals: mp 135-144 °C; ^{1}H NMR (400 MHz, THF-d_8) δ 1.63 (s, 12H), 1.78 (m, 16H), 3.62 (m, 16H), 6.63 (d, ^3J = 6.8 Hz, 2H), 6.71 (s, 1H), 7.02-7.08 (m, 3H), 7.19 (d, ^3J = 8.0 Hz, 2H),

7.28 (d, ^3J = 7.6 Hz, 2H); ^{13}C NMR (100 MHz, THF-d_8) δ 26.2 (t), 36.1 (q), 42.6 (s), 68.0 (t), 102.1 (d), 109.5 (d), 122.1 (d), 123.1 (d), 125.8 (d), 126.3 (d), 141.0 (s), 152.6 (s), 154.7 (s), two signals for the carbon atoms bound to the boron atom were not observed due to the quadrupolar relaxation; ^{7}Li NMR (155 MHz, THF-d_8) δ 0.51; ^{11}B NMR (128 MHz, THF-d_8) δ 30.4. The elemental analysis could not be performed due to the instability of the product toward air and moisture.

2. NMR Spectra
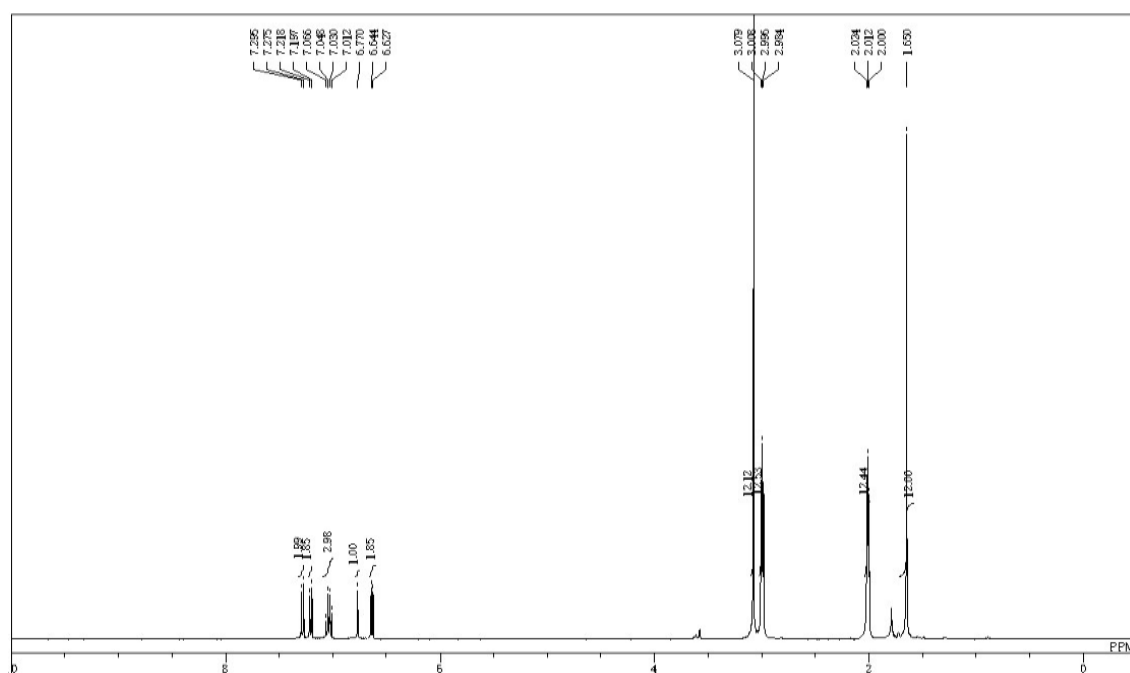
Figure S1. ^{1}H NMR spectrum of **2·K** in THF-d_8.
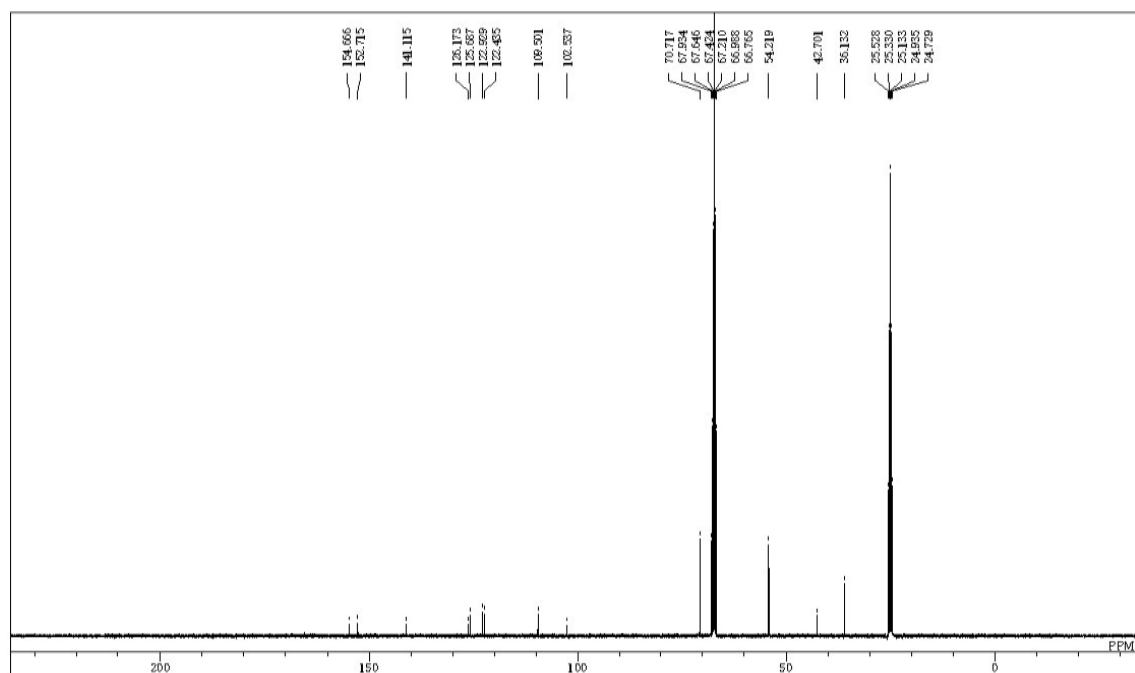
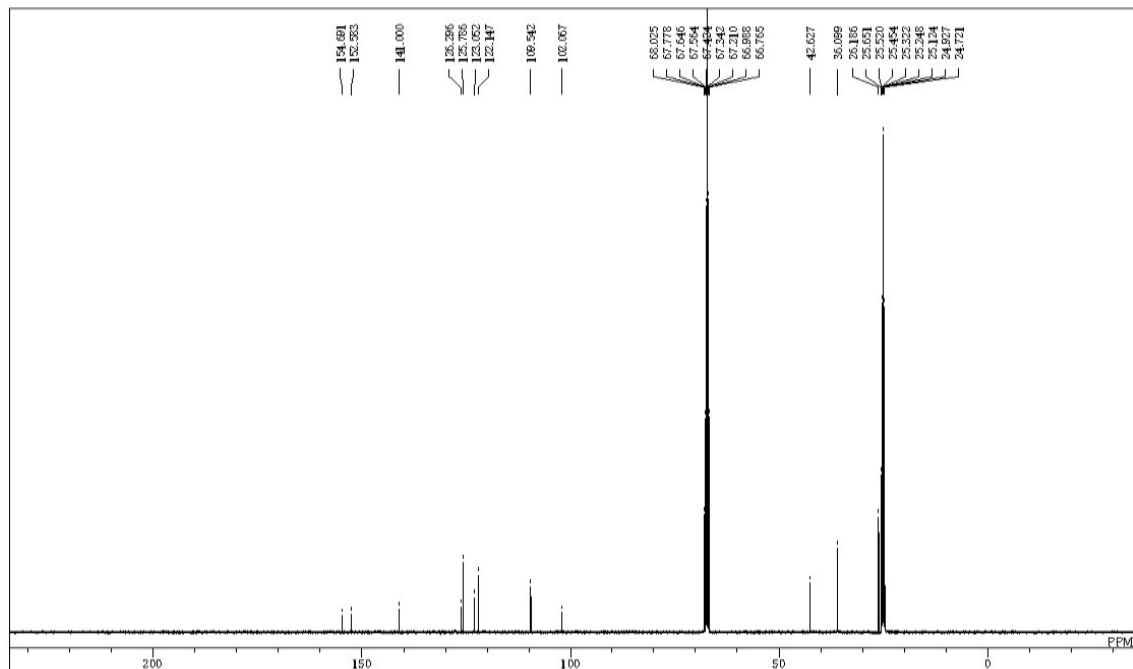**Figure S2.** ^{13}C NMR spectrum of **2·K** in THF-d_8.
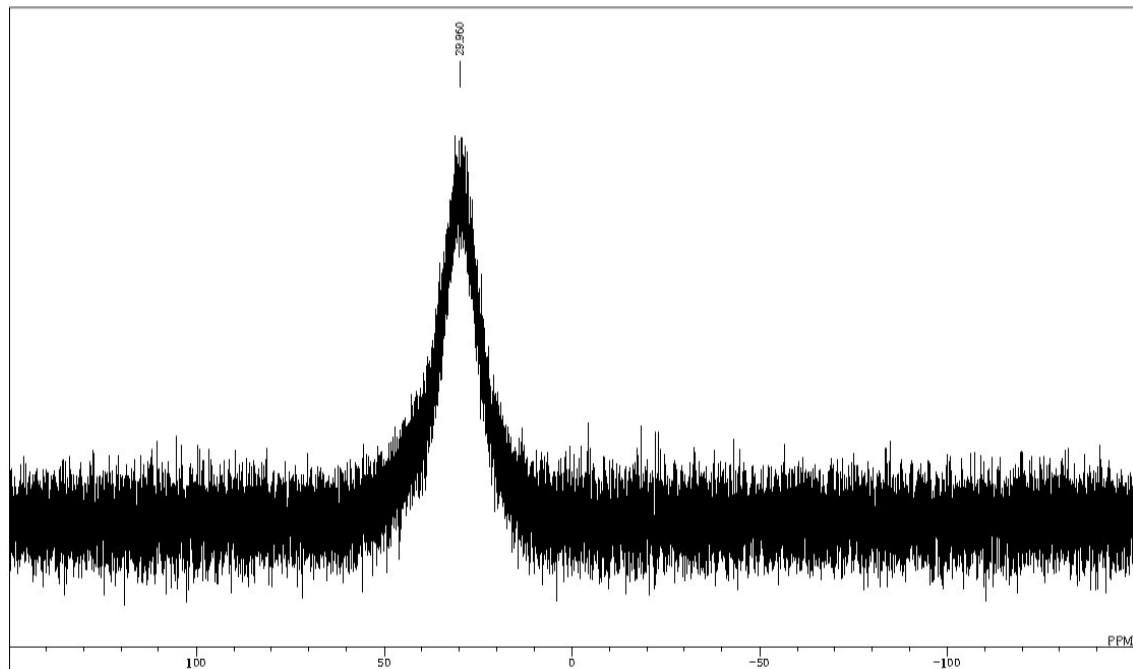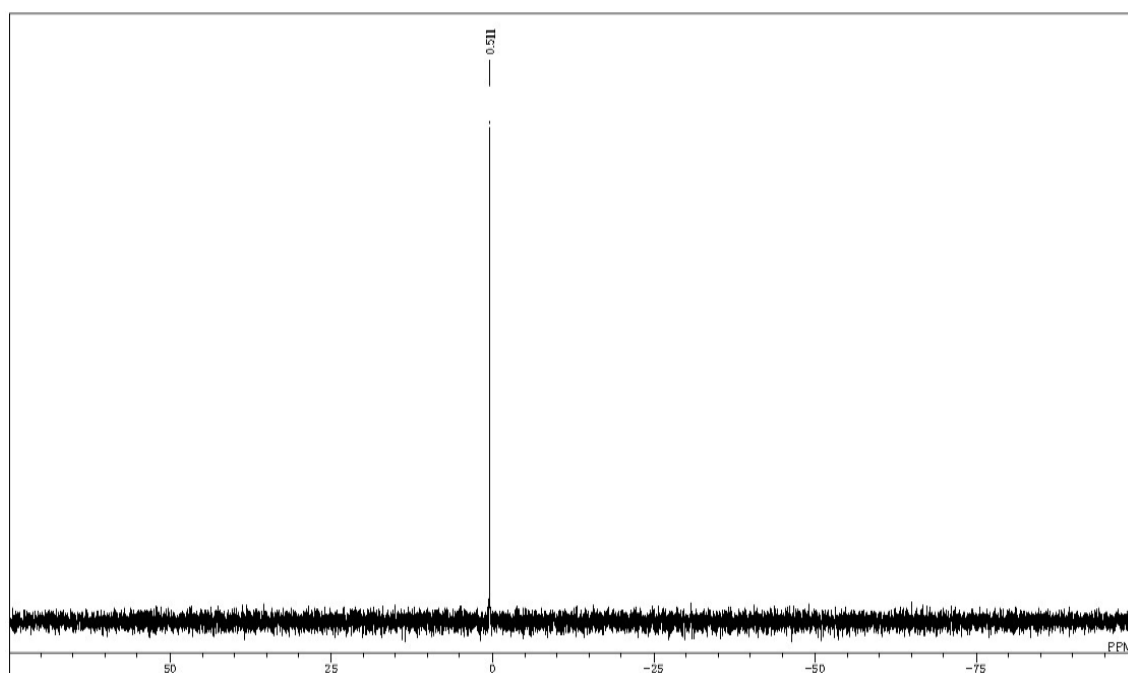

Figure S3. ^{11}B NMR spectrum of **2·K** in THF-d_8.
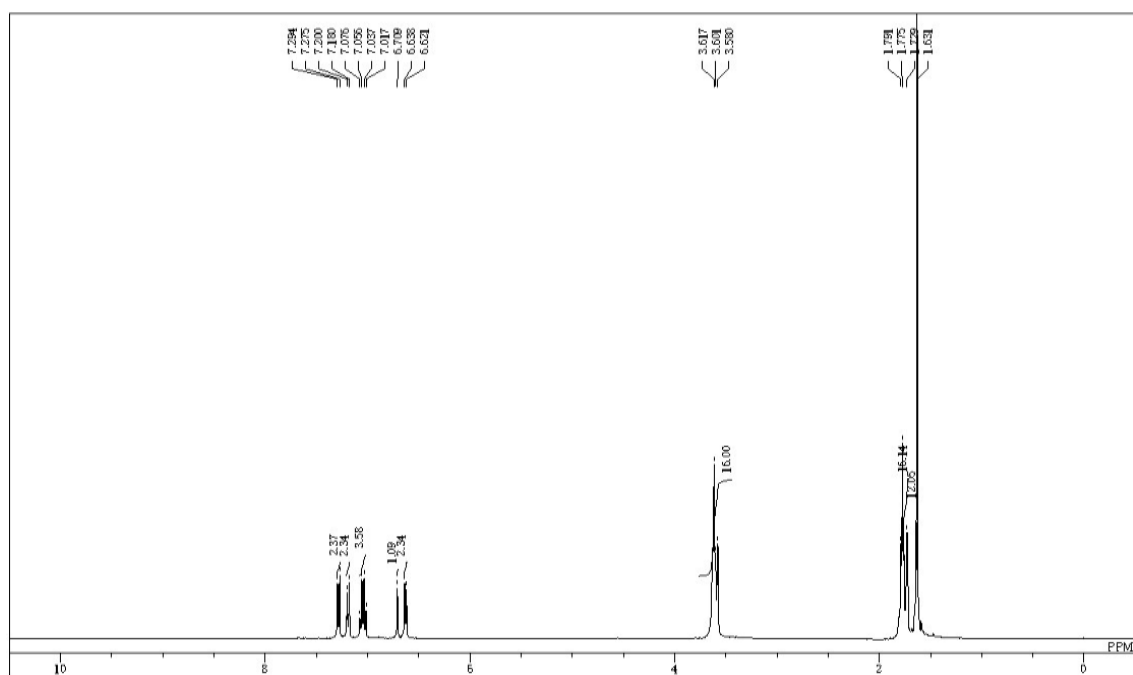
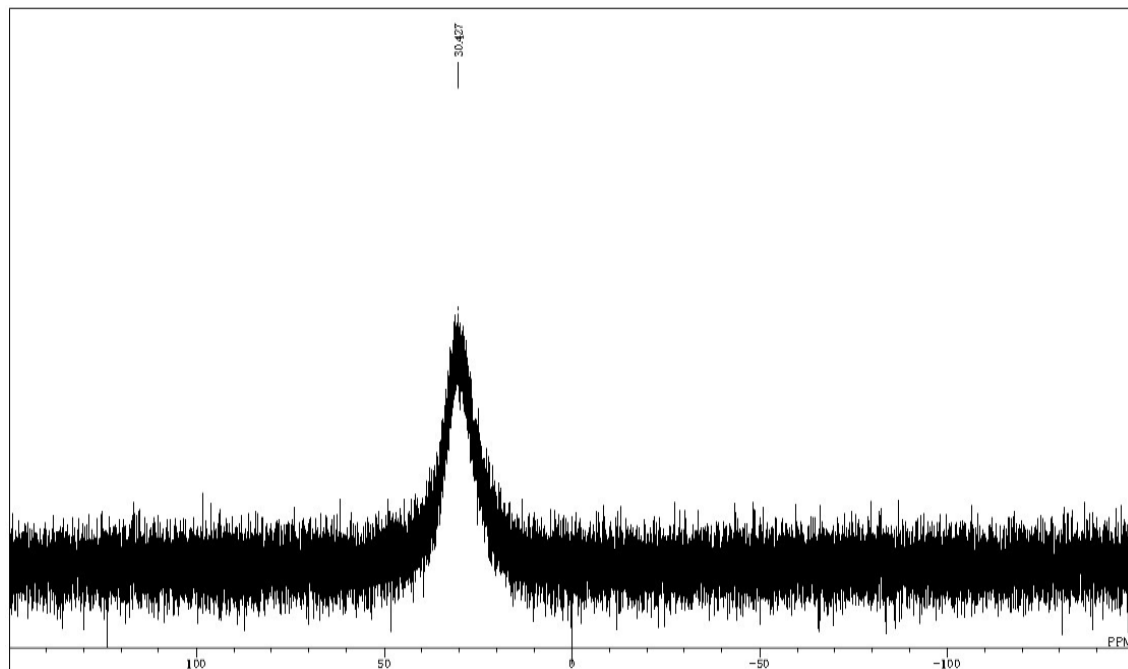**Figure S4.** ^{1}H NMR spectrum of **2·Li** in THF-d_8.

Figure S5. ^{13}C NMR spectrum of **2·Li** in THF-d_8.

S5

0.511

Figure S6. ^{7}Li NMR spectrum of **2·Li** in THF-d_8.

30.427

Figure S7. ^{11}B NMR spectrum of **2·Li** in THF-d_8.

3. Photophysical Properties

UV-visible absorption spectrum was recorded on a Shimadzu UV-3510 spectrometer. A sample solution (2.9×10^{-4} M) in a 1 mm quartz cell in degassed THF that were dried over NaK alloy was used for the measurement. Fluorescence spectrum was recorded on a Hitachi F-4500 spectrometer. Absolute fluorescence quantum yield was determined with a Hamamatsu C9920-02 calibrated integrating sphere system. THF solvent was dried over NaK alloy and degassed by three Freeze-Pump-Thaw cycles, then transferred into the sample in vacuo. A 1 cm square quartz cell including the sample solution was sealed before the measurement. Photophysical data of **2·K** are summarized in Table S1. The photophysical measurements of **2·Li** could not be performed due to the higher reactivity of **2·Li** to moisture compared to **2·K** in the highly diluted solutions. The lithium salt **2·Li** showed an orange emission and no noticeable difference from that of **2·K** was observed.

Table S1. Photophysical data of **2·K**

absorption		fluorescence	
λ_{abs}/nm	$\varepsilon/10^4$ M^{-1}cm^{-1}	λ_{fl}/nm	Φ_{fl}
568	3.67		
531	4.43	584	
500	2.79	591	0.45
412	4.83	634	
375	5.96		

4. X-Ray Crystallographic Analysis

Structural analysis of 1. The intensity data were collected on a Rigaku Saturn CCD diffractometer with graphite monochromator MoKα radiation ($\lambda = 0.71070$ Å) to $2\theta_{max} = 50°$ at 123 K. The structure was solved by direct methods (SHELXS-97)[2] and refined by full-matrix least-squares procedures on F^2 for all reflections (SHELXL-97).[2] While all hydrogen atoms were placed using AFIX instructions, all the other atoms were refined anisotropically. The crystal data are summarized in Table S2. The ORTEP drawing is shown in Figure S8. The data for selected bond lengths and angles are summarized in Table S3.

Table S2. Crystal data for **1**, **2·K**, and **2·Li**

	1	**2·K**	**2·Li**
CCDC ID code	895473	895474	895475
Empirical formula	$C_{25}H_{23}B$	$C_{43}H_{58}BKN_2O_6$	$C_{41}H_{54}BLiO_4$
Formula weight	334.24	748.82	628.59
Color	colorless	red	red
Crystal system	Orthorhombic	Monoclinic	Monoclinic
Space group	$C222_1$ (#20)	$P2_1/c$ (#14)	$P2_1/c$ (#14)
a (Å)	10.150(15)	23.898(8)	10.938(16)
b (Å)	17.72(3)	18.387(4)	34.75(3)
c (Å)	10.24(3)	18.78(2)	57.15(6)
β (deg)	90	104.083(17)	97.81(3)
V (Å^3)	1842(7)	8004(9)	21521(43)
Z	4	8	24
D_{calcd} (g cm^{-3})	1.205	1.243	1.164
$F(000)$	712	3216	8160
μ (mm^{-1})	0.067	0.182	0.072
Index range	$-12 \leq h \leq 12$	$-25 \leq h \leq 28$	$-11 \leq h \leq 12$
	$-20 \leq k \leq 20$	$-21 \leq k \leq 21$	$-37 \leq k \leq 39$
	$-12 \leq l \leq 11$	$-22 \leq l \leq 22$	$-65 \leq l \leq 65$
Reflections collected	6113	52851	97827
Independent reflections	1605 [R_{int} = 0.0500]	14066 [R_{int} = 0.0803]	31987 [R_{int} = 0.1087]
Goodness-of fit on F^2	0.969	1.151	1.085
R_1, wR_2 ($I>2\sigma(I)$)	0.0405, 0.0968	0.1028, 0.2467	0.1098, 0.2654
R_1, wR_2 (all data)	0.0466, 0.0994	0.1357, 0.2771	0.1963, 0.3531
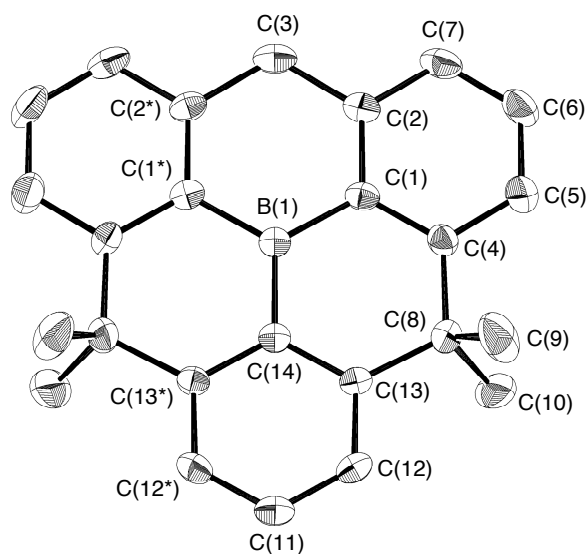
Figure S8. ORTEP drawing of **1** (50% probability for thermal ellipsoids). Hydrogen atoms are omitted for clarity.

Table S3. Selected bond lengths (Å) and angles (°) of **1**

B(1)–C(1)	1.519(3)	C(5)–C(6)	1.384(3)
B(1)–C(14)	1.525(4)	C(6)–C(7)	1.379(3)
C(1)–C(4)	1.402(3)	C(8)–C(9)	1.538(3)
C(1)–C(2)	1.414(3)	C(8)–C(13)	1.539(3)
C(2)–C(7)	1.381(3)	C(8)–C(10)	1.542(5)
C(2)–C(3)	1.513(3)	C(11)–C(12)	1.381(2)
C(4)–C(5)	1.398(3)	C(12)–C(13)	1.399(3)
C(4)–C(8)	1.541(3)	C(13)–C(14)	1.403(2)
C(1)–B(1)–C(1*)	120.7(2)	C(6)–C(7)–C(2)	119.96(19)
C(1)–B(1)–C(14)	119.63(11)	C(9)–C(8)–C(13)	108.29(19)
C(4)–C(1)–C(2)	120.67(16)	C(9)–C(8)–C(4)	107.76(15)
C(4)–C(1)–B(1)	120.18(17)	C(13)–C(8)–C(4)	115.63(16)
C(2)–C(1)–B(1)	119.10(16)	C(9)–C(8)–C(10)	110.20(19)
C(7)–C(2)–C(1)	119.44(17)	C(13)–C(8)–C(10)	107.84(18)
C(7)–C(2)–C(3)	119.85(19)	C(4)–C(8)–C(10)	107.08(16)
C(1)–C(2)–C(3)	120.71(16)	C(12*)–C(11)–C(12)	120.8(2)
C(2)–C(3)–C(2*)	119.6(2)	C(11)–C(12)–C(13)	120.60(18)

C(5)–C(4)–C(1)	118.18(18)	C(12)–C(13)–C(14)	118.15(17)
C(5)–C(4)–C(8)	119.58(17)	C(12)–C(13)–C(8)	118.71(15)
C(1)–C(4)–C(8)	122.23(16)	C(14)–C(13)–C(8)	123.14(17)
C(6)–C(5)–C(4)	120.62(19)	C(13)–C(14)–C(13*)	121.7(2)
C(7)–C(6)–C(5)	121.12(18)	C(13)–C(14)–B(1)	119.16(11)

Structural analysis of 2·K. The intensity data were collected on a Rigaku Saturn CCD diffractometer with graphite monochromator MoKα radiation ($\lambda = 0.71070$ Å) to $2\theta_{max} = 50°$ at 123 K. The structure was solved by direct methods (SHELXS-97)[2] and refined by full-matrix least-squares procedures on F^2 for all reflections (SHELXL-97).[2] While all hydrogen atoms were placed using AFIX instructions, all the other atoms were refined anisotropically. The crystal data are summarized in Table S2. The ORTEP drawing is shown in Figure S9. The data for selected bond lengths and angles are summarized in Table S4.
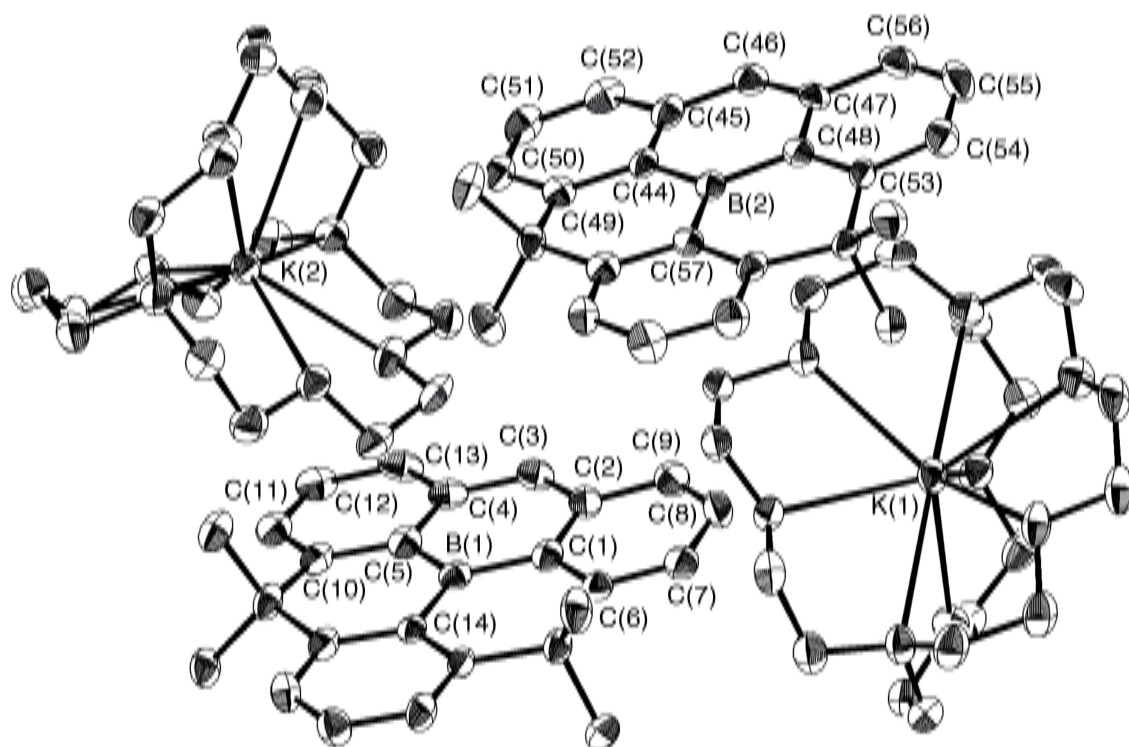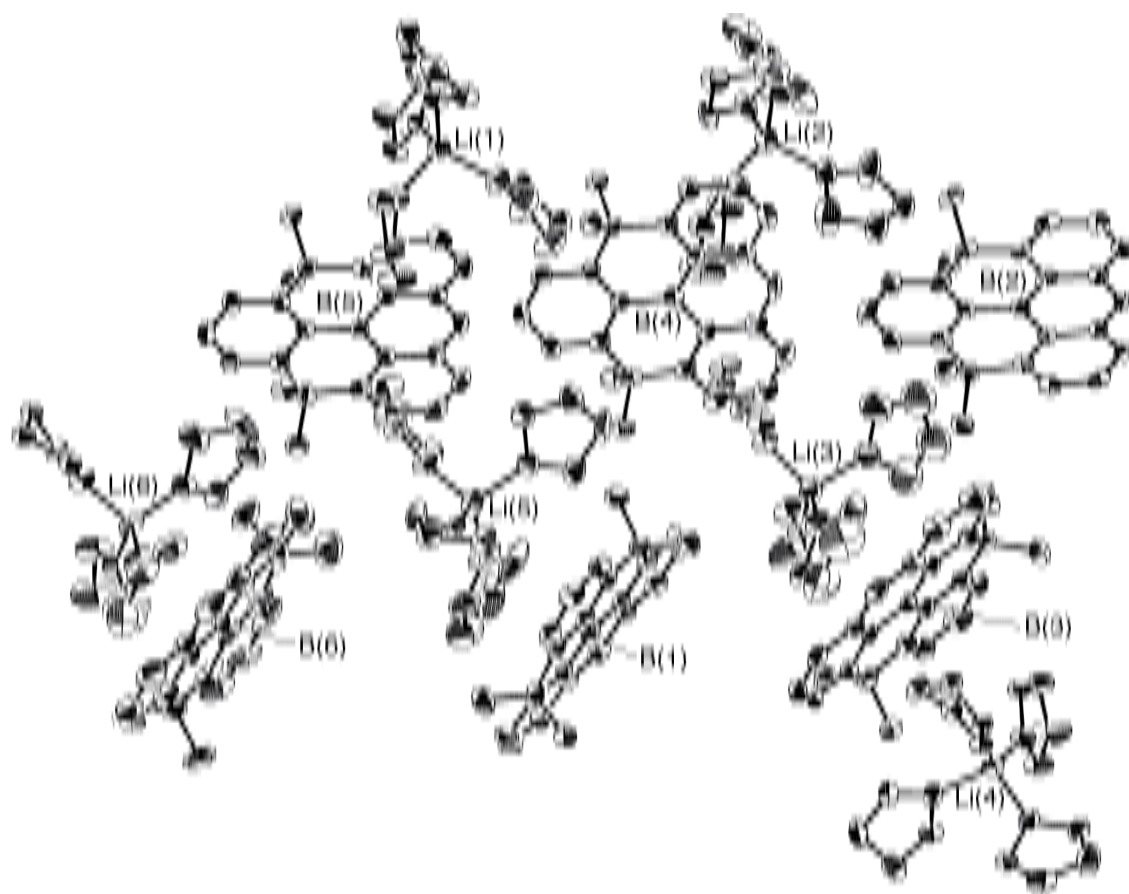

Figure S9. ORTEP drawing of **2·K** (50% probability for thermal ellipsoids). Hydrogen atoms are omitted for clarity. The crystal consists of two crystallographycally independent structures, whose structures are shown.
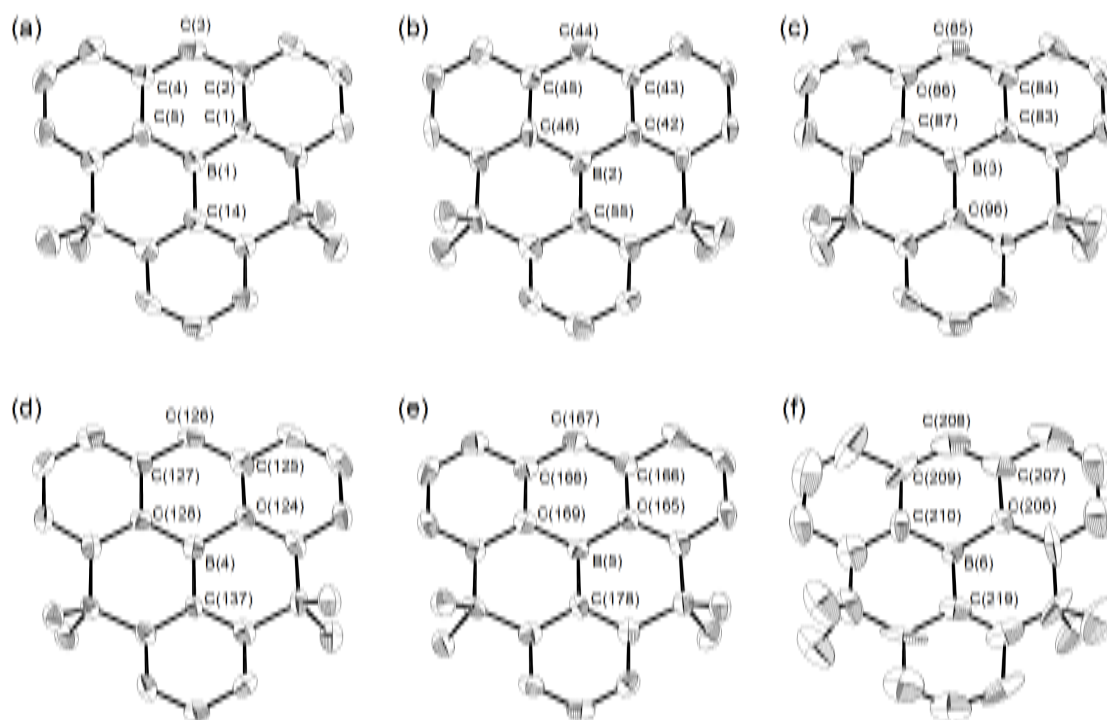
Table S4. Selected bond lengths (Å) and angles (°) of **2·K**

B(1)–C(1)	1.492(7)	B(2)–C(44)	1.502(7)
B(1)–C(5)	1.495(7)	B(2)–C(48)	1.495(7)
B(1)–C(14)	1.534(7)	B(2)–C(57)	1.520(7)
C(1)–C(6)	1.427(6)	C(44)–C(49)	1.420(6)
C(1)–C(2)	1.435(7)	C(44)–C(45)	1.438(7)
C(2)–C(3)	1.419(7)	C(45)–C(46)	1.411(7)
C(2)–C(9)	1.425(7)	C(45)–C(52)	1.426(6)
C(3)–C(4)	1.420(7)	C(46)–C(47)	1.409(7)
C(4)–C(5)	1.430(7)	C(47)–C(48)	1.430(7)
C(4)–C(13)	1.434(7)	C(47)–C(56)	1.436(6)
C(5)–C(10)	1.417(6)	C(48)–C(53)	1.413(6)
C(6)–C(7)	1.377(6)	C(49)–C(50)	1.374(6)
C(7)–C(8)	1.400(7)	C(50)–C(51)	1.422(7)
C(8)–C(9)	1.370(7)	C(51)–C(52)	1.364(7)
C(10)–C(11)	1.377(6)	C(53)–C(54)	1.385(7)
C(11)–C(12)	1.405(7)	C(54)–C(55)	1.404(7)
C(12)–C(13)	1.365(7)	C(55)–C(56)	1.369(7)
C(1)–B(1)–C(5)	119.7(4)	C(48)–B(2)–C(44)	119.3(4)
C(1)–B(1)–C(14)	120.6(4)	C(44)–B(2)–C(57)	120.0(4)
C(5)–B(1)–C(14)	119.7(4)	C(48)–B(2)–C(57)	120.7(4)
C(2)–C(1)–B(1)	119.0(4)	C(45)–C(44)–B(2)	118.4(4)
C(3)–C(2)–C(1)	119.3(4)	C(46)–C(45)–C(44)	119.9(4)
C(2)–C(3)–C(4)	123.4(4)	C(47)–C(46)–C(45)	123.2(4)
C(3)–C(4)–C(5)	120.6(4)	C(46)–C(47)–C(48)	121.0(4)
C(4)–C(5)–B(1)	117.9(4)	C(47)–C(48)–B(2)	117.9(4)

Structural analysis of 2·Li. The intensity data were collected on a Rigaku Saturn CCD diffractometer with graphite monochromator MoKα radiation ($\lambda = 0.71070$ Å) to $2\theta_{max} = 48°$ at 123 K. The structure was solved by direct methods (SHELXS-97)[2] and refined by full-matrix least-squares procedures on F^2 for all reflections (SHELXL-97).[2] While all hydrogen atoms were placed using AFIX instructions, all the other atoms were refined anisotropically. The crystal data are summarized in Table S2. The ORTEP drawing is shown in Figure S10. The ORTEP drawings of the anion part of each crystallographycally independent structure are shown in Figure S11. The data for selected bond lengths and angles are summarized in Table S5.

Figure S10. ORTEP drawing of **2·Li** (50% probability for thermal ellipsoids). Hydrogen atoms are omitted for clarity. The crystal consists of six crystallographycally independent structures, whose structures are shown.

Figure S11. ORTEP drawings of the anion part of six crystallographycally independent structures of **2·Li** (50% probability for thermal ellipsoids). Hydrogen atoms are omitted for clarity.

Table S5. Selected bond lengths (Å) and angles (°) of **2·Li**

B(1)–C(1)	1.488(9)	B(4)–C(124)	1.504(9)
B(1)–C(5)	1.492(9)	B(4)–C(128)	1.492(9)
B(1)–C(14)	1.529(9)	B(4)–C(137)	1.525(9)
C(1)–C(2)	1.437(8)	C(124)–C(125)	1.418(9)
C(2)–C(3)	1.420(9)	C(125)–C(126)	1.412(9)
C(3)–C(4)	1.407(9)	C(126)–C(127)	1.420(8)
C(4)–C(5)	1.436(8)	C(127)–C(128)	1.436(8)
B(2)–C(42)	1.496(9)	B(5)–C(165)	1.473(9)
B(2)–C(46)	1.496(9)	B(5)–C(169)	1.502(9)
B(2)–C(55)	1.526(9)	B(5)–C(178)	1.522(9)
C(42)–C(43)	1.443(8)	C(165)–C(166)	1.429(8)
C(43)–C(44)	1.418(8)	C(166)–C(167)	1.415(8)
C(44)–C(45)	1.403(8)	C(167)–C(168)	1.404(8)
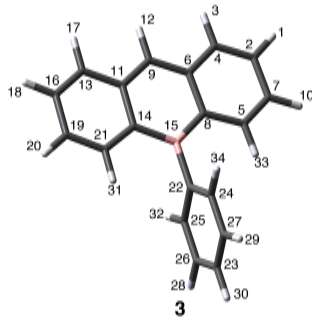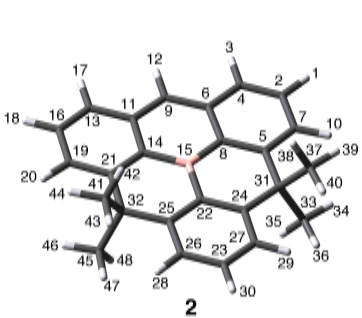
C(45)–C(46)	1.450(8)	C(168)–C(169)	1.441(8)
B(3)–C(83)	1.495(9)	B(6)–C(206)	1.489(9)
B(3)–C(87)	1.496(10)	B(6)–C(210)	1.494(9)
B(3)–C(96)	1.532(9)	B(6)–C(219)	1.491(9)
C(83)–C(84)	1.462(9)	C(206)–C(207)	1.432(9)
C(84)–C(85)	1.422(9)	C(207)–C(208)	1.340(11)
C(85)–C(86)	1.399(9)	C(208)–C(209)	1.399(11)
C(86)–C(87)	1.443(9)	C(209)–C(210)	1.459(11)
C(1)–B(1)–C(5)	119.5(6)	C(128)–B(4)–C(124)	118.4(6)
C(1)–B(1)–C(14)	120.0(6)	C(124)–B(4)–C(137)	121.8(6)
C(5)–B(1)–C(14)	120.4(6)	C(128)–B(4)–C(137)	119.8(6)
C(42)–B(2)–C(46)	119.6(6)	C(165)–B(5)–C(169)	118.9(6)
C(42)–B(2)–C(55)	119.7(5)	C(165)–B(5)–C(178)	120.9(6)
C(46)–B(2)–C(55)	120.7(6)	C(169)–B(5)–C(178)	120.2(5)
C(83)–B(3)–C(87)	120.0(6)	C(206)–B(6)–C(210)	118.2(6)
C(83)–B(3)–C(96)	119.6(6)	C(206)–B(6)–C(219)	120.5(6)
C(87)–B(3)–C(96)	120.4(6)	C(219)–B(6)–C(210)	121.2(6)

5. Theoretical Calculations

Natural population analysis (NPA). The NPA calculations of **2** and **3** were carried out using the Gaussian 03 program[3] at the B3LYP/6-31+G(d) level for the optimized structures obtained at the B3LYP/6-31+G(d) level.

**Table S6.** The NPA natural charges of **2** and **3** (B3LYP/6-31+G(d)//B3LYP/6-31+G(d))

	2			3	
atom	No.	charge	atom	No.	charge
H	1	0.21764	H	1	0.21677
C	2	–0.25125	C	2	–0.26266
H	3	0.21642	H	3	0.21566
C	4	–0.25385	C	4	–0.24232
C	5	0.03080	C	5	–0.18269
C	6	–0.02874	C	6	–0.03317
C	7	–0.30939	C	7	–0.32097
C	8	–0.34659	C	8	–0.38972
C	9	–0.29994	C	9	–0.30806
H	10	0.21281	H	10	0.21748
C	11	–0.02874	C	11	–0.04311
H	12	0.20649	H	12	0.20466
C	13	–0.25385	C	13	–0.22119
C	14	–0.34659	C	14	–0.38979
B	15	0.53930	B	15	0.58546
C	16	–0.25125	C	16	–0.27382
H	17	0.21642	H	17	0.21597

|					
H	18	0.21764	H	18	0.21676
C	19	–0.30939	C	19	–0.32087
H	20	0.21281	H	20	0.21744
C	21	0.03080	C	21	–0.18289
C	22	–0.27664	C	22	–0.26802
C	23	–0.26008	C	23	–0.27579
C	24	0.01409	C	24	–0.22864
C	25	0.01409	C	25	–0.22864
C	26	–0.25047	C	26	–0.25684
C	27	–0.25047	C	27	–0.25684
H	28	0.21981	H	28	0.22437
H	29	0.21981	H	29	0.22437
H	30	0.22245	H	30	0.22276
C	31	–0.11422	H	31	0.22770
C	32	–0.11422	H	32	0.23447
C	33	–0.65261	H	33	0.22771
H	34	0.22657	H	34	0.23447
H	35	0.24484	Total		–0.99999
H	36	0.21978			
C	37	–0.65261			
H	38	0.24484			
H	39	0.22657			
H	40	0.21978			
C	41	–0.65261			
H	42	0.24484			
H	43	0.21978			
H	44	0.22657			
C	45	–0.65261			
H	46	0.22657			
H	47	0.21978			
H	48	0.24484			
Total		–0.99999			

Nucleus independent chemical shift (NICS) calculations. The NICS calculations of **2** and **3** were carried out using the Gaussian 03 program[3] at the B3LYP/6-31+G(d) level for the optimized structures obtained at the B3LYP/6-31+G(d) level. The NICS values of $\mathbf{2'}_{//}$, $\mathbf{2'}_{\perp}$, $\mathbf{2'}$, $\mathbf{3}_{//}$, $\mathbf{3'}_{//}$, $\mathbf{3'}_{\perp}$, and $\mathbf{3'}$ were calculated using the corresponding geometries directly derived from the optimized structures of **2** and **3**.
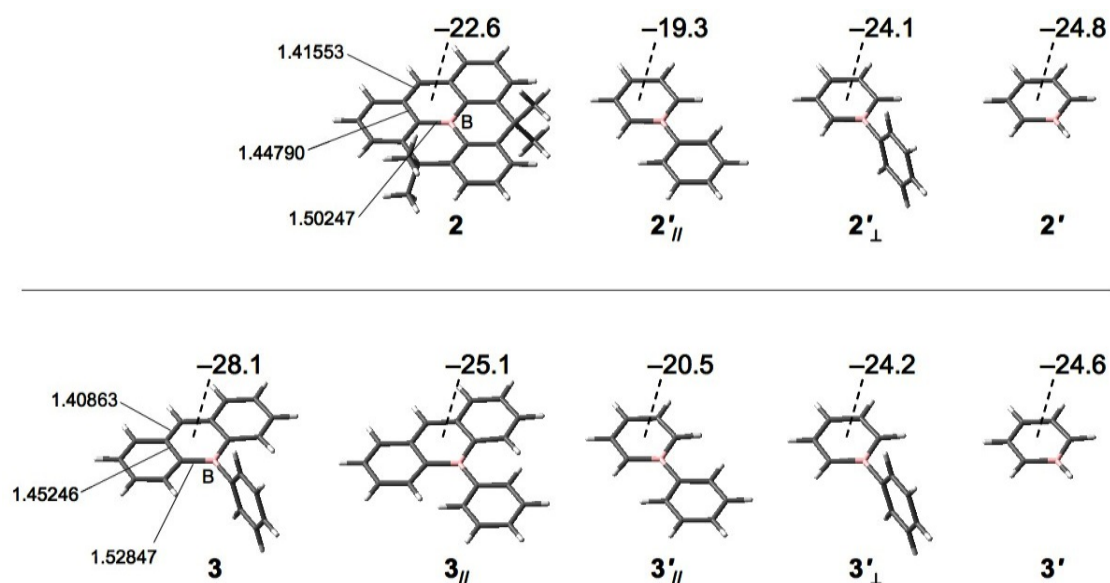
Figure S12. The $\mathrm{NICS(1)_{zz}}$ values for the boratabenzene ring of the optimized structures of **2** and **3**, and their substructures $\mathbf{2'}_{//}$, $\mathbf{2'}_{\perp}$, $\mathbf{2'}$, $\mathbf{3}_{//}$, $\mathbf{3'}_{//}$, $\mathbf{3'}_{\perp}$, and $\mathbf{3'}$, whose geometries are derived from the optimized structures of **2** and **3**, respectively. The selected bond lengths (Å) for the boratabenzene ring are given.

Time-dependent density functional theory (TD-DFT) calculations. The TD-DFT calculations of **2**, **3**$_\perp$, and **3**$_{//}$ with a cation were carried out using the Gaussian 03 program[3] at the B3LYP /6-31+G(d) level. The Structures of the anion parts were optimized at B3LYP/6-31+G(d) level, and then Li(OMe$_2$)$_3$ as the counter cation was fixed at 1.9 or 7.0 Å above the borataanthracene core.
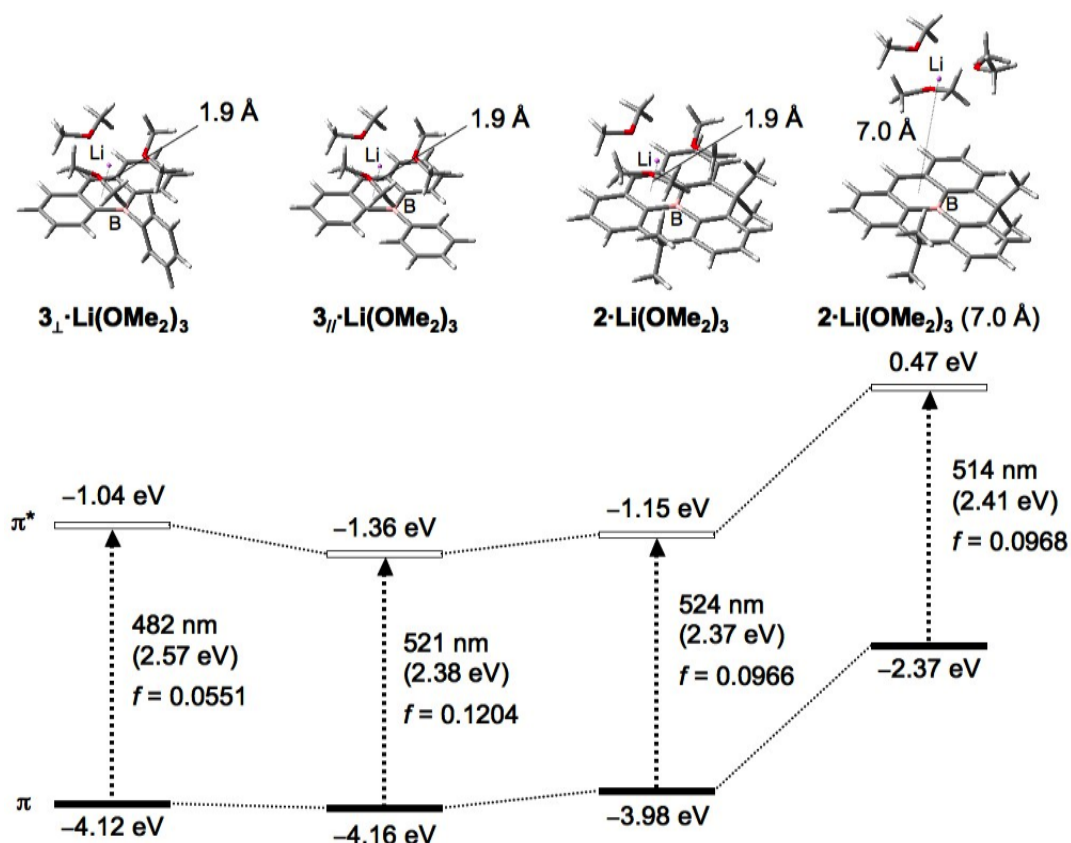
Figure S13. Comparison of the π and π* orbital energy levels, and the excitation energies among **2**, **3**$_\perp$, and **3**$_{//}$ with Li(OMe$_2$)$_3$ as the counter cation, based on the TD-DFT calculations at the B3LYP/6-31+G(d)//B3LYP/6-31+G(d) level.

6. References

1. Z. Zhou, A. Wakamiya, T. Kushida and S. Yamaguchi, *J. Am. Chem. Soc.*, 2012, **134**, 4529.

2. G. M. Sheldrick, *SHELX-97*, *Program for the Refinement of Crystal Structures*, University of Göttingen, Göttingen, Germany, 1997.

3. M. J. Frisch, G. W. Trucks, H. B. Schlegel, G. E. Scuseria, M. A. Robb, J. R. Cheeseman, J. A. Montgomery, Jr., T. Vreven, K. N. Kudin, J. C. Burant, J. M. Millam, S. S. Iyengar, J. Tomasi, V. Barone, B. Mennucci, M. Cossi, G. Scalmani, N. Rega, G. A. Petersson, H. Nakatsuji, M. Hada, M. Ehara, K. Toyota, R. Fukuda, J. Hasegawa, M. Ishida, T. Nakajima, Y. Honda, O. Kitao, H. Nakai, M. Klene, X. Li, J. E. Knox, H. P. Hratchian, J. B. Cross, C. Adamo, J. Jaramillo, R. Gomperts, R. E. Stratmann, O. Yazyev, A. J. Austin, R. Cammi, C. Pomelli, J. W. Ochterski, P. Y. Ayala, K. Morokuma, G. A. Voth, P. Salvador, J. J. Dannenberg, V. G. Zakrzewski, S. Dapprich, A. D. Daniels, M. C. Strain, O. Farkas, D. K. Malick, A. D. Rabuck, K. Raghavachari, J. B. Foresman, J. V. Ortiz, Q. Cui, A. G. Baboul, S. Clifford, J. Cioslowski, B. B. Stefanov, G. Liu, A. Liashenko, P. Piskorz, I. Komaromi, R. L. Martin, D. J. Fox, T. Keith, M. A. Al-Laham, C. Y. Peng, A. Nanayakkara, M. Challacombe, P. M. W. Gill, B. Johnson, W. Chen, M. W. Wong, C. Gonzalez, J. A. Pople, *Gaussian 03, Revision C.02*, Gaussian, Inc., Wallingford CT, 2004.